Theory of vortex force microscopy in superconducting layers

A. de la Cruz de Oña*

Department of Mathematics and Statistics, Concordia University, Montréal, Québec H3G 1M8, Canada

A. Badía-Majós

Departamento de Física de la Materia Condensada–ICMA, CPSUZ, María de Luna 3, E-50.018 Zaragoza, Spain

The interaction between a vortex within a finite-thickness type-II superconductor and a magnetic force microscopy tip is studied. By analyzing the expression of the arising lateral force, we show that the superconducting penetration depth may be recovered from experiment, using the so-called Laplace transform inversion method. This entails a vertical displacement experiment. The consideration of lateral scanning modes has allowed us to extend the theory to the more stable Hankel transform inversion method, which eventually becomes a Fourier analysis application. For the case of vortices in two-layered superconductors, we show that magnetic particle manipulation is possible by tuning the configuration of the layers.

I. INTRODUCTION

The interaction between superconducting materials and magnetic force microscopy (MFM) tips has been addressed in a number of recent studies. Thus, MFM has become a high-performance technique for the investigation of superconductors[1] as it offers the advantage of probing the London penetration depth λ within very small areas of the sample. This overcomes the difficulties associated to surface imperfections and inhomogeneities that can be hardly avoided in these materials. From the experimental point of view, the technique features more and more versatile operation.[2]

From the theoretical side, some remarkable advances refer to the still challenging inverse problem, i.e., recovering superconducting properties from observable quantities. In particular, the nondestructive evaluation of inhomogeneous penetration depth $\lambda(\vec{r})$,[3,4] and the concomitant difficulties related to finite-size effects,[5] have been dealt with. However, much of this work is only focused on Meissner state superconductors. The influence of vortices has been scarcely touched[6] and merely refers to the forward problem, i.e., prediction of the observables assuming the superconducting properties known. Remarkably, the presence of induced vortices may be either responsible for uncertainties in the interpretation of experiments,[7] or even a means of attempting the determination of λ.[8]

In this paper, we have developed an inverse method for recovering λ from the interaction between superconducting layers with vortices and MFM tips. The theory is developed for the lateral force arising when the tip settles over a flux quantum Φ_0. We recall that lateral forces, as well as dependence on the tip's lateral displacement, were not considered in previous studies. The planar translational invariance for superconducting layers in the Meissner state produces a magnetostatic interaction which only depends on the vertical distance. However, with vortices present, the horizontal position of the tip plays a role. Taking advantage of this, we will

show that inversion techniques may be extended and improved. Thus, horizontal scanning will be related to Fourier-Bessel transforms, which are quite well behaved as compared to previous proposals.

It is of note that lateral force microscopy (LFM) is already possible by means of a new generation of cantilevers, which are sensitive to the force in any direction. To be specific, this is achieved with the so-called domain wall tips, described in Refs. 9 and 10.

The existence of a maximum in the lateral force versus distance curve has been predicted. This feature, together with the consideration of two-layered superconductors, has inspired the proposal of magnetic particle manipulation by means of vortex microscopy. In brief, a potential well for lateral displacements is formed upon the vortex. The barrier shape may be tuned by changing the separation between the superconductors. Thus, one can either trap or release nanometric particles settling on the top layer, by vertical displacement of the underlying one. This concept is basically reciprocal to recent ideas for obtaining controlled movement of vortices and other entities by means of nanomagnets or magnetic bubble systems[9–12] and microcoils.[13]

Although our investigation was focused on the action of the vortex field upon the magnetic particle, a number of complimentary quantities, such as the full magnetic field distribution and superconducting current density, are derived. Here, they have been used for the assessment of the physical results, but may also be the basis for further studies.

The work is organized as follows. In Sec. II, we study the forward and inverse problems related to the vortex force microscopy (VFM) on a superconducting layer. In Sec. III, we use the London theory for analyzing the behavior of a vortex within a superconducting bi-layer. The interaction with a force microscopy tip is also analyzed. Finally, inspired by the arising physical scenario, Sec. IV is devoted to the proposal of a mechanism for manipulating small magnetic particles by the action of vortex fields in layered systems.

II. VFM ON A SUPERCONDUCTING LAYER

A. Forward problem

1. Stray field of the vortex

In this section, we solve the magnetostatic boundary value problem in a type-II superconducting thin film with a vortex. The superconductor is parallel to the XY plane, and fills the space between $z=0$ and $z=-b$. This selection allows to reproduce previous results[6,14] in a somewhat more compact form, and eases comparison with bilayers. As it is customary, vorticity is incorporated to the London theory by means of a two-dimensional impulse (delta) function centered at the position where the vortex settles ($\rho_0=0$) for simplicity. Then, if one follows the convention for the fields in the domains of interest

$$\vec{h}_v = \begin{cases} \vec{h}_1(\vec{r}), & z > 0 \\ \vec{h}_2(\vec{r}), & -b < z < 0 \\ \vec{h}_3(\vec{r}), & z < -b, \end{cases} \quad (1)$$

it follows that

$$\nabla^2 \vec{h}_1 = 0,$$

$$\nabla^2 \vec{h}_2 - (1/\lambda^2)\vec{h}_2 = -\frac{\Phi_0}{\lambda^2}\delta_2(\rho)\mathbf{e}_z,$$

$$\nabla^2 \vec{h}_3 = 0. \quad (2)$$

Now, one can benefit from the problem's symmetry in order to simplify the differential equation statement. Thus, using the two-dimensional Fourier transform

$$\vec{\mathcal{H}}(\vec{k},z) = \frac{1}{2\pi}\int_\forall d^2\vec{r}\, e^{-i\vec{k}\cdot\vec{\rho}}\vec{h}(\rho,z), \quad (3)$$

we get the simplified system

$$\partial_z^2\vec{\mathcal{H}}_1 - k^2\vec{\mathcal{H}}_1 = 0,$$

$$\partial_z^2\vec{\mathcal{H}}_2 - \gamma^2\vec{\mathcal{H}}_2 = -\frac{\Phi_0}{\lambda^2}\mathbf{e}_z,$$

$$\partial_z^2\vec{\mathcal{H}}_3 - k^2\vec{\mathcal{H}}_3 = 0, \quad (4)$$

with the well-known solution

$$\vec{\mathcal{H}}_1 = \vec{\mathcal{V}}_1(k)e^{-kz},$$

$$\vec{\mathcal{H}}_2 = \vec{\mathcal{V}}_2^+(k)\cosh(\gamma z) + \vec{\mathcal{V}}_2^-(k)\sinh(\gamma z) + \frac{\Phi_0\mathbf{e}_z}{2\pi\gamma^2\lambda^2},$$

$$\vec{\mathcal{H}}_3 = \vec{\mathcal{V}}_3(k)e^{k(z+b)}. \quad (5)$$

Above, we have used $\gamma \equiv \sqrt{k^2+1/\lambda^2}$. Mathematically valid solutions that correspond to unphysically divergent fields have been rejected.

In order to obtain the coefficients $\vec{\mathcal{V}}(k)$, one must impose continuity boundary conditions on the planar interfaces $z=0,-b$. This leads to

$$\mathcal{V}_{1z}(k) = \gamma\Delta\{\gamma\sinh(b\gamma) + k[\cosh(b\gamma)-1]\}, \quad (6a)$$

$$\mathcal{V}_{2z}^+(k) = -k\Delta\{k\sinh(b\gamma) + \gamma[\cosh(b\gamma)+1]\}, \quad (6b)$$

$$\mathcal{V}_{2z}^-(k) = -k\Delta\{\gamma\sinh(b\gamma) + k[\cosh(b\gamma)-1]\}, \quad (6c)$$

$$\mathcal{V}_{3z}(k) = \gamma\Delta\{\gamma\sinh(b\gamma) + k[\cosh(b\gamma)-1]\}, \quad (6d)$$

where

$$\Delta \equiv \frac{\Phi_0/2\pi\gamma^2\lambda^2}{2k\gamma\cosh(b\gamma) + (k^2+\gamma^2)\sinh(b\gamma)}.$$

Finally, one can express the components of the magnetic field by inverting the Fourier transform, i.e.,

$$h_z(\rho,z) = \frac{1}{2\pi}\int_\forall d^2\vec{k}\, e^{i\vec{k}\cdot\vec{\rho}}\,\mathcal{H}_z(k,z)$$

$$= \frac{1}{2\pi}\int_0^\infty dk\left[\int_0^{2\pi}d\phi\, e^{ik\rho\,\cos(\phi)}\right]k\mathcal{H}_z(k,z)$$

$$= \int_0^\infty dk\, J_0(k\rho)k\mathcal{H}_z(k,z). \quad (7)$$

Here, J_0 stands for the zeroth-order Bessel function of the first kind. Schläfli's integral representation of this function has been recalled. Thus, we obtain

$$h_{1z}(\rho,z) = \int_0^\infty dk\, kJ_0(k\rho)\mathcal{V}_{1z}(k)e^{-kz}, \quad (8a)$$

$$h_{2z}(\rho,z) = \int_0^\infty dk\, kJ_0(k\rho)[\mathcal{V}_{2z}^+(k)\cosh(\gamma z) + \mathcal{V}_{2z}^-(k)\sinh(\gamma z)]$$

$$+ \frac{\Phi_0}{2\pi\lambda^2}K_0\left(\frac{\rho}{\lambda}\right), \quad (8b)$$

$$h_{3z}(\rho,z) = \int_0^\infty dk\, kJ_0(k\rho)\mathcal{V}_{3z}(k)e^{k(z+b)}, \quad (8c)$$

with K_0 the zeroth-order modified Bessel function of the second kind. These equations allow the straightforward evaluation of some related physical quantities. In particular, if one uses the divergenless character of the magnetic field, together with the cylindrical symmetry of our problem, the relation

$$\frac{\partial}{\partial\rho}(\rho h_\rho) = -\rho\frac{\partial h_z}{\partial z} \quad (9)$$

may be used for determining the field component h_ρ by quadrature. Then, the supercurrent density within the superconductor $j_\theta(\rho,-b \leq z \leq 0)$ can be derived from Ampere's law,

$$j_\theta(\rho,z) = \frac{c}{4\pi}\left[\frac{\partial h_\rho}{\partial z} - \frac{\partial h_z}{\partial \rho}\right]. \tag{10}$$

This leads to

$$j_\theta = -\frac{c}{4\pi\lambda^2}\int_0^\infty dk\, J_1(k\rho)[\mathcal{V}_{2z}^+(k)\cosh(\gamma z) + \mathcal{V}_{2z}^-(k)\sinh(\gamma z)]$$

$$+ \frac{c\,\Phi_0}{8\pi^2\lambda^3}K_1\!\left(\frac{\rho}{\lambda}\right). \tag{11}$$

2. Vortex-tip interaction

The physical quantities considered above allow us to evaluate the interaction between the vortex and the MFM tip. In particular, we are interested in the mutual magnetic force. This may be derived from the appropriate *free energy* of the system, which is analyzed below.

First, we recall that the amount of energy related to the creation of a current density distribution is[15]

$$\mathcal{U}_{\vec{j}} = \frac{1}{2c}\int_\forall \vec{j}\cdot\vec{A}\,dV = \frac{1}{8\pi}\int_\forall B^2\,dV. \tag{12}$$

This term accounts for the work done against electromotive forces, and may be considered as a *potential energy*. When dealing with superconductors, one must additionally include a *kinetic energy* term, related to the charge carriers, which takes the form

$$\mathcal{U}_k = \frac{2\pi}{c^2}\int_s \lambda^2 j_s^2\,dV. \tag{13}$$

Thus, the magnetic energy $\mathcal{U}=\mathcal{U}_{\vec{j}}+\mathcal{U}_k$ becomes

$$\mathcal{U} = \frac{1}{2c}\int_\forall \vec{j}\cdot\vec{A}\,dV + \frac{1}{8\pi}\int_s \lambda^2\|\nabla\times\nabla\times\vec{A}\|^2\,dV. \tag{14}$$

Now, the suitable free energy, related to virtual displacements of the permanent magnet, is[15]

$$\mathcal{F} = \mathcal{U} - \frac{1}{c}\int_m \vec{j}_m\cdot\vec{A}\,dV. \tag{15}$$

Here, we introduce the fact that magnetization current densities remain unchanged.

Above, subindices s,m have been used, respectively, for the superconductor and the magnet. The quantities with no subindex correspond to the superposition of both contributions.

Equation (15) may be given a practical form by using London's equation,

$$\vec{A} + \lambda^2\nabla\times\nabla\times\vec{A} = \vec{\Phi}_v. \tag{16}$$

In the case of one vortex present in the layer, the vorticity term becomes $\vec{\Phi}_v = (0,\Phi_0/2\pi\rho,0)$ in cylindrical coordinates. Thus, one gets

$$\mathcal{F} = \frac{1}{2c}\int_s \vec{\Phi}_v\cdot\vec{j}_s\,dV - \frac{1}{2c}\int_m \vec{j}_m\cdot\vec{A}\,dV. \tag{17}$$

Next, we split up the supercurrents as $\vec{j}_s = \vec{j}_{me} + \vec{j}_v$, indicating the superposition of induced Meissner currents, and the vortex contribution. We have

$$\mathcal{F} = \frac{1}{2c}\int_s (\vec{\Phi}_v\cdot\vec{j}_v + \vec{\Phi}_v\cdot\vec{j}_{me})dV - \frac{1}{2c}\int_m (\vec{j}_m\cdot\vec{A}_s + \vec{j}_m\cdot\vec{A}_m)dV. \tag{18}$$

Substracting the constant self-interaction energies $\vec{\Phi}_v\cdot\vec{j}_v$ and $\vec{j}_m\cdot\vec{A}_m$, and using the symmetry of the mutual interaction terms, one gets

$$\widetilde{\mathcal{F}} \equiv \mathcal{F} - \frac{1}{2c}\int_s \vec{\Phi}_v\cdot\vec{j}_v\,dV - \frac{1}{2c}\int_m \vec{j}_m\cdot\vec{A}_m\,dV$$

$$= \frac{1}{2c}\int_s (\vec{\Phi}_v\cdot\vec{j}_{me} - \vec{j}_v\cdot\vec{A}_m - \vec{j}_{me}\cdot\vec{A}_m)dV. \tag{19}$$

Eventually, one can use the equality of the first two terms, which represent the interaction between the vortex and the Meissner currents, and the interaction between the vortex and the magnet.[16] The free energy becomes

$$\widetilde{\mathcal{F}} = -\frac{1}{c}\int_s \vec{j}_v\cdot\vec{A}_m\,dV - \frac{1}{2c}\int_s \vec{j}_{me}\cdot\vec{A}_m\,dV, \tag{20}$$

or, by virtue of symmetry,

$$\widetilde{\mathcal{F}} = -\frac{1}{c}\int_m \vec{j}_m\cdot\vec{A}_v\,dV - \frac{1}{2c}\int_m \vec{j}_m\cdot\vec{A}_{me}\,dV. \tag{21}$$

Eventually, the application of vector analysis formulas leads to the alternative expression

$$\widetilde{\mathcal{F}} = -\int_m \vec{M}\cdot\vec{h}_v\,dV - \frac{1}{2}\int_m \vec{M}\cdot\vec{h}_{me}\,dV \equiv \mathcal{F}_v(a,\vec{\rho}) + \mathcal{F}_{me}(a). \tag{22}$$

Above, $\mathcal{F}_v$ stands for the magnet-vortex interaction and $\mathcal{F}_{me}$ for the interaction with the induced Meissner currents. $(a,\vec{\rho})$ are used for the vertical and lateral coordinates of the magnetic tip (see below). In the general case, one should account for both terms in order to evaluate the interaction forces between the magnet and the superconductor. However, as we will focus on the lateral force, only the first term plays a role, i.e.,

$$\vec{F}_L(a,\vec{\rho}) = -\frac{\partial\widetilde{\mathcal{F}}}{\partial\vec{\rho}} = -\frac{\partial\mathcal{F}_v}{\partial\vec{\rho}}. \tag{23}$$

This expression may be readily evaluated for the case of a dipole tip $\vec{m}=(0,0,m_z)$, settling at the point (ρ,θ,a) above the vortex. The radial force is
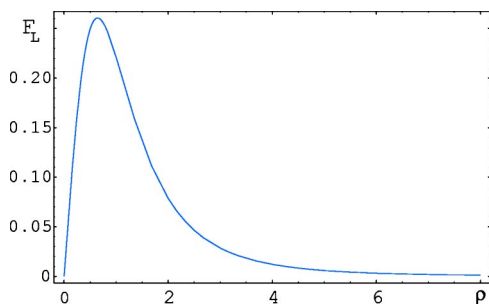
FIG. 1. The lateral force $F_L(a_0,\rho)$ curves as a function of the lateral distance ρ, using a point dipole approximation for the tip. Here we have taken $\lambda=0.2, b=0.1, a_0=1$. See Sec. II A 3 for the units.

$$F_L(a,\rho) = -\frac{\partial(-\vec{m}\cdot\vec{h}_1)}{\partial\rho} = -m_z\int_0^\infty dk\, k^2 \mathcal{V}_{1z}(k)e^{-ka}J_1(k\rho).$$
(24)

Equation (24) may be generalized so as to incorporate size effects for the tip by means of superposition. However, lateral displacements entail a complex vector summation, because the unit vector $\hat{\rho}$ is different for each volume element. This is not a shortcoming for numerical evaluations, but in order to bring out the physics with the least mathematical complication we confine to analytical evaluations in what follows. On the other hand, these calculations fit the possibility of investigating the superconducting properties by using the dipole of microsquids or domain-wall tips.

Based on the previous equations, Fig. 1 displays the dependence of the lateral force $F_L(a_0,\rho)$ as a function of the lateral distance ρ for a point dipole. Notice the maximum at some distance from the center of the vortex. Figure 2 shows the graph of the lateral force versus the vertical distance $F_L(a,\rho_0)$ for a given lateral distance. We recall that the observed behavior is the same as that reported in Ref. 17, where the assumption $b\ll\lambda$ was used.

3. Quantitative evaluation: Physical units

The following convention will be used throughout the paper for quantitative evaluations. First, we determine the length units by selecting a definite value for the film thick-
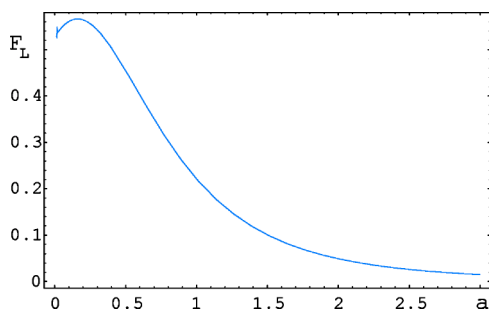

FIG. 2. The lateral force $F_L(a,\rho_0)$ curves as a function of the vertical distance a, using a point dipole approximation for the tip. Here we have taken $\lambda=0.2, b=0.1, \rho_0=1$. See Sec. II A 3 for the units.

ness, i.e., $b=0.2$ means $b=0.2\,\ell$. The coefficients $\mathcal{V}$ are given in units of the flux quantum, i.e., $\mathcal{V}=0.5$ means $\mathcal{V}=0.5\,\Phi_0/2\pi$. Finally, the force is expressed in units of $m\,\Phi_0\,\ell^3$, with m the magnetic moment of the tip. Specific values for a particular experiment may be obtained by choosing the associated ℓ and m.

B. Inverse problem

Below, we present the theory for inverse vortex force microscopy. It will be shown that both the superconducting penetration depth and the thickness of the film may be recovered by the Laplace transform inversion method, which was already applied to superconductors in the Meissner state. In addition, the consideration of lateral displacements has inspired a novel and intrinsically more stable technique, the so-called Hankel inversion method. Eventually, the combination of both techniques is also suggested.

As concerns the thickness of the superconducting film, we want to emphasize that it may be accurately obtained by other methods, as electron microscopy or Rutherford backscattering. Thus, our proposed magnetic determination may be used in combination with them, as a self-consistency check.

1. Laplace transform inversion method

Laplace transformation inspired methods were initially suggested in half-space geometry for recovering the penetration depth λ in superconductors with no vortices present.[4] Further generalization[5] allowed us to consider thin superconductors, even with unknown thickness b. Here, we show that VFM also allows us to recover the pair (λ, b) by the same algorithm. The method will be implemented for the lateral forces.

Recall the definition of the Laplace transform operator $\mathcal{L}[f(k)](a) = \int \exp(-ak)f(k)dk$. Then, Eqs. (24) may be written as

$$F_L(a,\rho_0) = -m_z\mathcal{L}[k^2\mathcal{V}_{1z}(k)J_1(k\rho_0)](a).$$
(25)

Notice that above, ρ is to be considered as a parameter, while the distance a is the *Laplace transformed* variable. This mathematical concept has a clear physical counterpart. The associated experiment consists of a vertical scanning, while lateral displacements are not allowed. Subsequent data analysis will be made for the pairs $[a_i, F_L(a_i)]$ and a given value for ρ_0.

Eventually, one can formally apply the inverse operator $\mathcal{L}^{-1}$ and obtain

$$\mathcal{V}_{1z}(k) = -\frac{1}{m_z k^2 J_1(k\rho_0)}\mathcal{L}^{-1}[F_L(a,\rho_0)](k)$$

$$\equiv -\frac{S(k,\rho_0)}{k^2}\mathcal{L}^{-1}[F_L(a,\rho_0)](k).$$
(26)

Recalling that $\mathcal{V}_{1z}(k)$ depends on λ and b, one can use the previous equation in order to devise an operational relation involving these quantities and experimental or computable data. Suppose that we need to determine the pair (λ, b) from
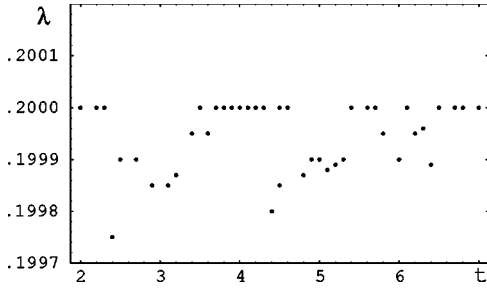
FIG. 3. Recovery of the London penetration depth λ by VFM, using $F_L(a)$ for the case of simulated experiment with $(\lambda,b) = (0.2,0.1)$. A magnetic dipole approximation was used for the tip. λ is plotted as a function of the wave-number ratio $t = k_2/k_1$.

FIG. 4. Recovery of the superconducting slab thickness b by VFM, using $F_L(a)$ for the case of simulated experiment with $(\lambda,b) = (0.2,0.1)$. A magnetic dipole approximation was used for the tip. b is plotted as a function of the wave-number ratio $t = k_2/k_1$.

the available information, $\mathcal{L}^{-1}[F_L(a,\rho_0)](k)$, for a collection of values of the wave number k. Equation (26) may be written as

$$g(k;\lambda,b) = \frac{S(k)}{k^2}\mathcal{L}^{-1}[F_L(a,\rho_0)](k) + \mathcal{V}_{1z}(k) = 0. \quad (27)$$

Considering the wave number k as a parameter, we can take any couple of nontrivial values $k_1 \neq k_2$ and pose the following nonlinear system of equations:

$$\frac{S(k_1)}{k_1^2}\mathcal{L}^{-1}[F_L(a,\rho_0)](k_1) + \mathcal{V}_{1z}(k_1) = 0,$$

$$\frac{S(k_2)}{k_2^2}\mathcal{L}^{-1}[F_L(a,\rho_0)](k_2) + \mathcal{V}_{1z}(k_2) = 0, \quad (28)$$

or in a compact form

$$g_1(k;\lambda,b) = 0,$$

$$g_2(k;\lambda,b) = 0, \quad (29)$$

where $k \equiv k_1$ and $g_2(k;\lambda,b) = g_1(tk;\lambda,b)$ provided $t = k_2/k_1$.

This kind of nonlinear equation system is analogous to the one that appears in the resolution of the inverse MFM problem for superconductors without vortices, and magnetic materials in Refs. 5 and 18. We have applied the previous procedure for simulated noise corrupted data. A random noise, corresponding to 0.1% resolution of the measured force, has been added (see Ref. 19 for further details). Figures 3 and 4 show the recovered quantities λ and b from our artificial data. The graphs were obtained for the lateral force on a VFM dipole tip.

It is of note that the above kind of inverse problem is ill-posed, with difficulties of nonuniqueness and instability of the solution. This stems from the fact that Laplace transform inversion is intrinsically unstable and small variations in the initial conditions may cause large variations in the solutions. On the other hand, our simulation was performed under the assumption that the VFM data are available for all distances between the tip and the vortex position. It is apparent that this would be restricted by the experimental conditions. As a final technical remark, we recall that Laplace transform inversion of real data is an even more delicate task, because, contrary to the case of faked data, complex-
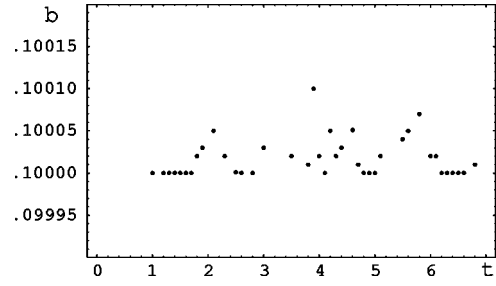
variable-based algorithms cannot be used. Although real-value-based methods are at hand, application is not trivial and no single method gives optimum results for all purposes. For instance, the commonly used Gaver-Stehfest method[20] is based on a series expansion, whose accuracy does not increase with the number of terms N, owing to numerical rounding errors. Thus, one must choose an optimum value of N which depends on the machine precision.

2. Hankel transform inversion method

In this subsection, we show that the consideration of lateral displacements for the VFM tip allows us to introduce an interesting concept, which allows us to skip the mathematical difficulties explained above. Thus, if one performs a horizontal scanning for a given distance between the tip and the superconducting film, data inversion relates to a more simple and well-behaved mathematical operation, i.e., the so-called Hankel transform inversion. Furthermore, the close relation between Hankel and Fourier transforms allows us to use the latter, which is a widespread mathematical application. Again, we start with Eqs. (24). Now, we recall the definition of the Hankel transform operator $H_1[f(k)](\rho) = \int kJ_1(k\rho)f(k)dk$. This allows us to write

$$F_L(a_0,\rho) = -m_z H_1[k\mathcal{V}_{1z}(k)e^{-ka_0}](\rho). \quad (30)$$

Here, our point of view is complimentary to the previous paragraph. The distance a_0 is to be considered as a parameter, and ρ is the *Hankel transformed* variable. The proposed experiment would consist of a horizontal scanning, while keeping a constant vertical distance between the tip and the superconducting layer. Mathematical inversion should be performed for the pairs $[\rho_i, F_L(\rho_i)]$. To be specific, one can apply the inverse operator H_1^{-1} and obtain

$$\mathcal{V}_{1z}(k) = -\frac{e^{ka_0}}{m_z k}H_1^{-1}[F_L(a_0,\rho)](k)$$

$$\equiv -\frac{T(k,a_0)}{k^2}H_1^{-1}[F_L(a_0,\rho)](k). \quad (31)$$

It is apparent that the method for recovering (λ,b), which was described in the framework of Laplace inversion for vertical displacement modes, may be literally translated to this case. One gets the system
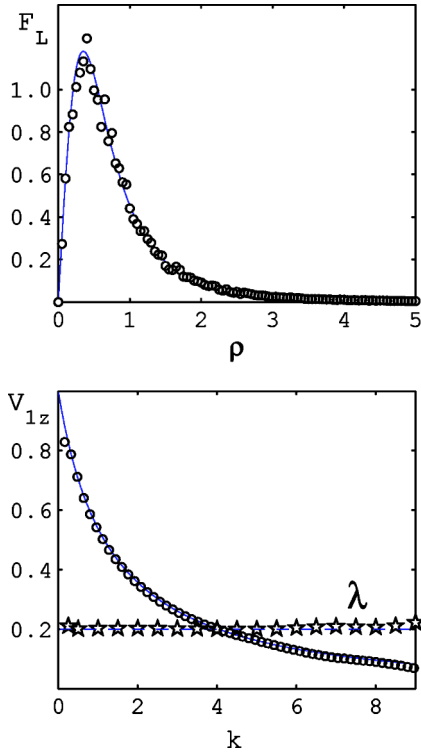
FIG. 5. Recovery of the superconducting penetration depth from the Hankel transform technique. The upper panel shows the theoretical lateral force (continuous line) as well as a simulated measurement (symbols). The lower panel displays the theoretical value of the coefficient $\mathcal{V}_{1z}$ as well as its recovery from experiment (symbols). The stars are used for the recovered λ. $(\lambda, b) = (0.2, 0.1)$ and $a_0 = 0.5$ was used for our faked data. See Sec. II A 3 for the units.

$$\frac{T(k_1)}{k_1^2} H_1^{-1}[F_L(a_0, \rho)](k_1) + \mathcal{V}_{1z}(k_1) = 0,$$

$$\frac{T(k_2)}{k_2^2} H_1^{-1}[F_L(a_0, \rho)](k_2) + \mathcal{V}_{1z}(k_2) = 0, \qquad (32)$$

which allows us to obtain the superconducting properties from experimental data. Again, we have applied the previous procedure for simulated noise corrupted data. Figure 5 displays the results. It is of note that even for moderate noise levels (10% in this case), λ can be recovered in a nonsmall range of wave-number values k.

We want to stress that Hankel transform inversion overcomes the technical difficulties related to the Laplace transform. The fundamental mathematical issue is the celebrated inversion theorem $H_\mu^{-1} = H_\mu$, i.e., the forward and inverse transformations have the same operational form (in our case $\mu = 1$). This is customarily expressed in terms of the δ function as

$$\int_0^\infty d\rho \, \rho J_\mu(\rho k) J_\mu(\rho k') = \frac{\delta(k - k')}{k'}$$

$$\Updownarrow$$

$$H_\mu^{-1} = H_\mu.$$

In conclusion, the inversion algorithm is more stable and allows us to introduce real-valued data without complication.

As a final remark, and tracing back to Eq. (7), the one-dimensional Hankel transform stated above may be cast as a two-dimensional Fourier transform. In fact,

$$H_1^{-1}[F_L(a_0, \rho)](k) = \mathcal{F}_2^{-1}[F_L(a_0, \rho)\Psi_1(x, y)](k). \qquad (33)$$

Here, we have used

$$\rho \equiv \sqrt{x^2 + y^2},$$

$$\Psi_1(x, y) \equiv -\frac{ix + y}{\sqrt{x^2 + y^2}}. \qquad (34)$$

This equivalence may be of interest because a variety of optimal and robust fast Fourier transform algorithms are at hand.

3. Hybrid Laplace-Hankel inversion method

We want to emphasize that vertical and lateral displacement modes could be used in combination. In practice, a vertical scanning for a given value ρ_1, as well as a lateral scanning for a given height a_1, are suggested. The selection of a_1 and ρ_1 relies on experimental resolution considerations. For example, inspired by Figs. 1 and 2, one could settle close to the maxima. Eventually, the inversion equations are

$$\frac{S(k)}{k^2} \mathcal{L}^{-1}[F_L(a, \rho_1)](k) + \mathcal{V}_{1z}(k) = 0,$$

$$\frac{T(k)}{k^2} H_1^{-1}[F_L(a_1, \rho)](k) + \mathcal{V}_{1z}(k) = 0. \qquad (35)$$

III. VFM ON SUPERCONDUCTING BILAYERS

A. Forward problem

Here, we develop the theory for the magnetostatic interaction between a magnetic tip and the vortex field, when a second superconducting layer is introduced. To be specific, the vortex settles within the upper layer, of thickness b and penetration depth λ_1. A half-space with penetration depth λ_2 lies below, which will modify the flux structure spreading out from the vortex. The governing London equations of the problem read

$$\nabla^2 \vec{h}_1 = 0,$$

$$\nabla^2 \vec{h}_2 - (1/\lambda_1^2)\vec{h}_2 = -\frac{\Phi_0}{\lambda_1^2} \delta_2(\rho)\mathbf{e}_z,$$

$$\nabla^2 \vec{h}_3 - (1/\lambda_2^2)\nabla^2 \vec{h}_3 = 0. \qquad (36)$$

Notice that vorticity has been limited to the upper medium. Proceeding as in the case of a single superconducting layer [Eqs. (3)–(6)], we have the Fourier components

$$\vec{\mathcal{H}}_1(k,z) = \vec{\mathcal{D}}_1(k)e^{-kz},$$

$$\vec{\mathcal{H}}_2(k,z) = \vec{\mathcal{D}}_2^+(k)\cosh(\gamma_1 z) + \vec{\mathcal{D}}_2^-(k)\sinh(\gamma_1 z) + \frac{\Phi_0 \mathbf{e}_z}{2\pi\gamma_1^2\lambda_1^2},$$

$$\vec{\mathcal{H}}_3(k,z) = \vec{\mathcal{D}}_3(k)e^{\gamma_2(z+b)}, \qquad (37)$$

where $\gamma_i \equiv \sqrt{k^2 + 1/\lambda_i^2}$ and $i = 1,2$.

Again, recalling continuity boundary conditions at the interfaces $z=0$ and $z=-b$, we obtain

$$\mathcal{D}_{1z}(k) = \gamma_1 \Delta_2 \{\gamma_1 \sinh(b\gamma_1) + k[\cosh(b\gamma_1) - 1]\}, \qquad (38a)$$

$$\mathcal{D}_{2z}^+(k) = -k\Delta_2 \left\{ \gamma_2 \sinh(b\gamma_1) + \gamma_1\left[\cosh(b\gamma_1) + \frac{\gamma_2}{k}\right]\right\}, \qquad (38b)$$

$$\mathcal{D}_{2z}^-(k) = -k\Delta_2 \{\gamma_1 \sinh(b\gamma_1) + \gamma_2[\cosh(b\gamma_1) - 1]\}, \qquad (38c)$$

$$\mathcal{D}_{3z}(k) = \gamma_1 \Delta_2 \{\gamma_1 \sinh(b\gamma_1) + k[\cosh(b\gamma_1) - 1]\}, \qquad (38d)$$

where

$$\Delta_2 \equiv \frac{\Phi_0/2\pi\gamma_1^2\lambda_1^2}{(\gamma_1\gamma_2 + \gamma_1 k)\cosh(b\gamma_1) + (\gamma_1^2 + \gamma_2 k)\sinh(b\gamma_1)}.$$

We want to notice that all the results in Sec. II can be obtained from the limit $\gamma_2 \to k$, which is nothing but considering a large penetration depth in the second medium $\lambda_2 \to \infty$. Eventually, Fourier transform inversion leads to

$$h_{1z}(\rho,z) = \int_0^\infty dk\, kJ_0(k\rho)\mathcal{D}_{1z}(k)e^{-kz}, \qquad (39a)$$

$$h_{2z}(\rho,z) = \int_0^\infty dk\, kJ_0(k\rho)[\mathcal{D}_{2z}^+(k)\cosh(\gamma_1 z)$$
$$+ \mathcal{D}_{2z}^-(k)\sinh(\gamma_1 z)] + \frac{\Phi_0}{2\pi\lambda_1^2}K_0\left(\frac{\rho}{\lambda_1}\right), \quad (39b)$$

$$h_{3z}(\rho,z) = \int_0^\infty dk\, kJ_0(k\rho)\mathcal{D}_{3z}(k)e^{\gamma_2(b+z)}. \qquad (39c)$$

Now, using the same technique presented in Sec. II [Eqs. (9) and (10)], one may obtain the supercurrent density distribution in both media,

$$j_{1,\theta} = -\frac{c}{4\pi\lambda_1^2}\int_0^\infty dk\, J_1(k\rho)[\mathcal{D}_{2z}^+(k)\cosh(\gamma_1 z)$$
$$+ \mathcal{D}_{2z}^-(k)\sinh(\gamma_1 z)] + \frac{c\,\Phi_0}{8\pi^2\lambda_1^3}K_1\left(\frac{\rho}{\lambda_1}\right), \quad (40)$$

$$j_{2,\theta} = -\frac{c}{4\pi\lambda_2^2}\int_0^\infty dk\, J_1(k\rho)\mathcal{D}_{3z}(k)e^{\gamma_2(b+z)}. \qquad (41)$$

Vortex-tip interaction

The interaction between a magnetic point dipole tip $\vec{m} = (0,0,m_z)$ located at (ρ,θ,a) and the vortex at the origin of the cylindrical coordinate system may be evaluated in the same manner as in Sec. II. One gets

$$F_L(a,\rho) = -\frac{m_z\Phi_0}{2\pi}\int_0^\infty dk\, k^2\mathcal{D}_{1z}(k)e^{-ka}J_1(k\rho). \qquad (42)$$

B. Inverse problem

In principle, one can perform an analysis completetely parallel to the one discussed in Sec. II B for the case of single-layer superconductors. However, in this case, a new equation must be included for solving the triple (λ_1,λ_2,b). To be specific, one should either solve the system

$$\frac{S(k_1)}{k_1^2}\mathcal{L}^{-1}[F_L(a,\rho_0)](k_1) + \mathcal{D}_{1z}(k_1) = 0,$$

$$\frac{S(k_2)}{k_2^2}\mathcal{L}^{-1}[F_L(a,\rho_0)](k_2) + \mathcal{D}_{1z}(k_2) = 0,$$

$$\frac{S(k_3)}{k_3^2}\mathcal{L}^{-1}[F_L(a,\rho_0)](k_3) + \mathcal{D}_{1z}(k_3) = 0 \qquad (43)$$

for vertical displacement modes, or

$$\frac{T(k_1)}{k_1^2}\mathrm{H}_1^{-1}[F_L(a_0,\rho)](k_1) + \mathcal{D}_{1z}(k_1) = 0,$$

$$\frac{T(k_2)}{k_2^2}\mathrm{H}_1^{-1}[F_L(a_0,\rho)](k_2) + \mathcal{D}_{1z}(k_2) = 0,$$

$$\frac{T(k_3)}{k_3^2}\mathrm{H}_1^{-1}[F_L(a_0,\rho)](k_3) + \mathcal{D}_{1z}(k_3) = 0 \qquad (44)$$

for lateral dispacement modes.

IV. MICROMAGNETIC PARTICLE MANIPULATION

In this section, we report on how one could manipulate the position of magnetic particles by tuning the vortex-particle interaction lateral force. Here, we will focus our attention on a single particle and a single vortex, but the idea is valid for an assembly of particles, settling above an Abrikosov lattice of vortices as well. In this latter case, one could even produce a forth and back creep of particles.

Let us suppose that a vortex is pinned within a superconducting layer of penetration depth λ_1. Let the magnetic particle settle in equilibrium above the vortex as a result of the balance between some external force and the lateral interaction $F_L(a,\rho)$ described in this work. Just by adding a second superconducting material whose separation to the first is
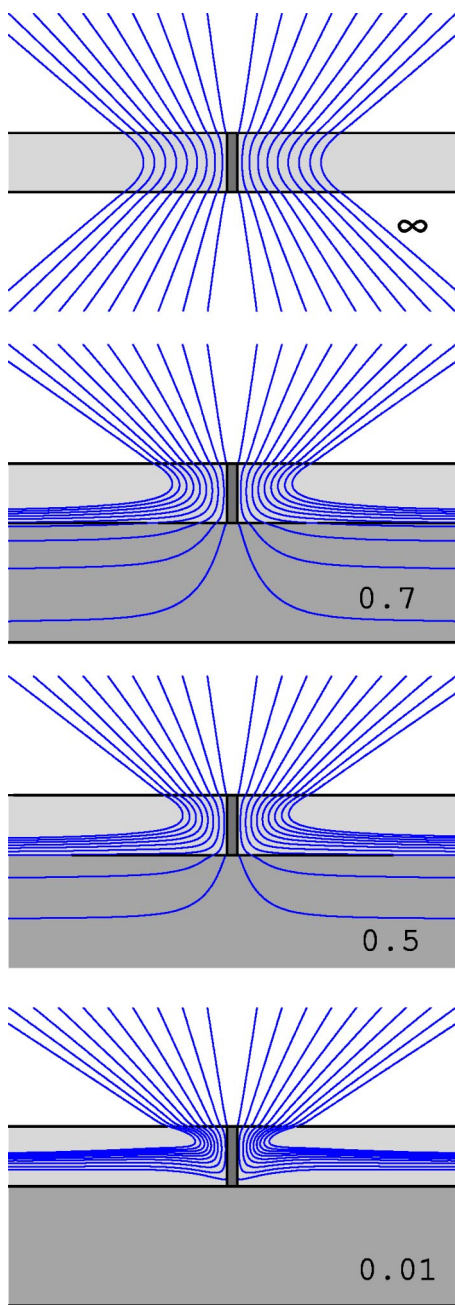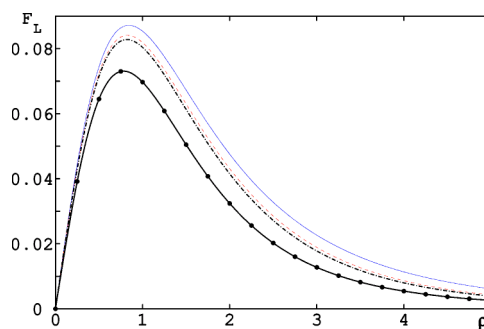
FIG. 7. The lateral force $F_L(a_0,\rho)$ for several values of λ_2 (0.7, 0.5, and 0.01 in descending order of the curves). The upper curve (continuous line) represents the limit $\lambda_2 \to \infty$. λ_1 was taken to be 0.9, the slab thickness $b=1$, and the vertical distance $a_0=1$. See Sec. II A 3 for the details about units.

As a final remark, we want to comment on the effect of the upper superconducting layer thickness. Figure 8 shows the results for the lateral force in the cases of a single and double layer. Notice that for a single layer, the force increases with b because the stray field is confined to a smaller region and $\partial h_{1,z}/\partial\rho$ increases. However, the effect of adding a second superconducting layer is more prominent when the thickness b diminishes.

V. CONCLUSION

Along this work, we have developed the theoretical background for the recovery of the penetration depth λ in superconductors with vortices, by force microscopy experiments. Namely, we present the concept of vortex force microscopy, i.e., the physical interaction between the flux quantum and a tiny magnetic particle. It is shown that λ may be recovered from lateral force detection. In addition, this quantity may be recorded either as a function of the tip-sample vertical distance a, or horizontally scanning above the vortex. The latter mode was not described in previous studies, owing to the *XY* translational invariance of the vertical force in Meissner state layers. Outstandingly, the horizontal scanning mode relates to a quite well-behaved inverse problem, as compared to the
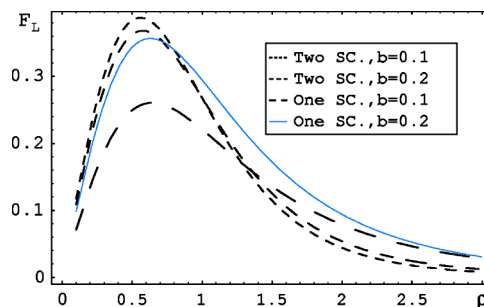

FIG. 6. Vortex field lines for a single-layer (top) and a double-layer superconductor with decreasing values of the penetration depth in the second medium λ_2, as labeled to the bottom of the plots. $(\lambda_1,b)=(0.9,1.0)$ was used for the upper layer.

made smaller and smaller, the lateral force is reduced and the particle may be released. As an alternative which avoids the intrinsic difficulties of cryogenic mechanical operation, we also suggest to use temperature control. Thus, one could thermally isolate both layers and take advantage of the variation $\lambda_2(T)$.

The phenomenon is illustrated by Figs. 6 and 7. We recall that the action of the lower superconducting layer is to push the vortex field lines from below. Such compression reduces the lateral variation $\partial h_{1,z}/\partial\rho$ and the force F_L diminishes. As is apparent from both figures, the effect is more and more pronounced as λ_2 diminishes.

FIG. 8. The lateral force $F_L(a_0,\rho)$ as a function of the lateral distance ρ for a system composed of one or two superconductors. The behavior for two values of the superconducting layer thickness b is included. The dipole approximation has been used for the tip. $\lambda_1=\lambda_2$ was taken to be 0.2, and the vertical distance $a_0=1$. See Sec. II A 3 for the details about units.

ill-posed vertical case. In brief, lateral displacement data must be treated by a Hankel transform, instead of the unstable inverse Laplace transform for vertical scanning. Furthermore, a close relation exists between Hankel and Fourier transforms. This allows the numerical implementation of a widespread collection of robust Fourier transform algorithms.

By analyzing the vortex field in two-layered superconductors, one is led to the proposal of a simple means of manipulating magnetic particles. It has been shown that adding a superconducting layer beneath the one which holds the vortex stretches out the stray field above the superconductors. Then, the lateral force F_L exerted on a magnetic particle that stays in equilibrium in that region diminishes and, eventually, it may be released.

As a final potential application of vortex force microscopy, we want to mention the study of magnetic films and nanostructures[21,22] by scanning the interaction with the vortex field. The sharp variation of the field intensity, as well as the fluxoid quantization condition, encourage the proposed experiments as the basis for quantitative magnetic force microscopy.

ACKNOWLEDGMENTS

*Electronic address: artorde@vax2.concordia.ca

[1] H. J. Hug, Th. Jung, H. J. Güntherodt, and H. Thomas, Physica C **175**, 375 (1991); H. J. Reittu and R. Laiho, Semicond. Sci. Technol. **5**, 448 (1992); A. Wadas, O. Fritz, H. J. Hug, and H. J. Güntherodt, Z. Phys. B: Condens. Matter **88**, 317 (1992); H. J. Hug, A. Moser, I. Parashikov, B. Stiefel, O. Fritz, H. J. Güntherodt, and H. Thomas, Physica C **2695**, 235 (1994); A. Moser, H. J. Hug, O. Fritz, I. Parashikov, and H. J. Güntherodt, J. Vac. Sci. Technol. B **12**, 1586 (1994); A. Moser, H. J. Hug, I. Parashikov, B. Stiefel, O. Fritz, H. Thomas, A. Baratoff, H. J. Güntherodt, and P. Chaudhari, Phys. Rev. Lett. **74**, 1847 (1995); A. Volodin, K. Temst, C. Van Haesendonck, and Y. Bruynseraede, Appl. Phys. Lett. **73**, 1134 (1998).

[2] H. J. Hug, B. Stiefel, P. J. A. Vanschendel, A. Moser, S. Martin, and H. J. Güntherodt, Rev. Sci. Instrum. **70**, 3625 (1999).

[3] M. W. Coffey, Phys. Rev. Lett. **83**, 1648 (1999).

[4] M. W. Coffey, Phys. Rev. B **57**, 11 648 (1998).

[5] A. Badía, Phys. Rev. B **63**, 094502 (2001).

[6] M. W. Coffey and E. T. Phipps, Phys. Rev. B **53**, 389 (1996).

[7] M. Roseman, P. Grütter, A. Badía, and V. Metlushko, J. Appl. Phys. **89**, 6787 (2001).

[8] M. Roseman and P. Grütter, New J. Phys. **3**, 24.1 (2001).

[9] L. E. Helseth, T. H. Johansen, and T. M. Fischer, Phys. Rev. Lett. **91**, 208302 (2003).

[10] P. E. Goa, H. Hauglin, A. A. Olsen, D. Shantsev, and T. H. Johansen, Appl. Phys. Lett. **82**, 79 (2003).

[11] L. E. Helseth, Phys. Rev. B **66**, 104508 (2002); L. E. Helseth, P. E. Goa, H. Hauglin, M. Baziljevich, and T. H. Johansen, *ibid.* **65**, 132514 (2002).

[12] L. E. Helseth, Phys. Lett. A **315**, 399 (2003); **319**, 413 (2003).

[13] B. W. Gardner, J. C. Wynn, D. A. Bonn, R. Liang, W. N. Hardy, J. R. Kirtley, V. G. Kogan, and K. A. Moler, Appl. Phys. Lett. **80**, 1010 (2002).

[14] M. V. Milŏsević, S. V. Yampolskiĭ, and F. M. Peeters, Phys. Rev. B **66**, 174519 (2002).

[15] L. D. Landau and E. M. Lifshitz, *Theoretical Physics*, Vol. 8, Electrodynamics of Continuous Media, 2nd ed. (Pergamon, Oxford, 1984).

[16] M. V. Milŏsević and F. M. Peeters, Phys. Rev. B **68**, 094510 (2003).

[17] J. C. Wei, J. L. Chen, L. Horng, and T. J. Yang, Phys. Rev. B **54**, 15 429 (1996).

[18] A. de la Cruz de Oña, Physica B **348**, 177 (2004).

[19] A. Badía, Phys. Rev. B **60**, 10 436 (1999).

[20] M. W. Coffey, Inverse Probl. **15**, 669 (1999); D. P. Gaver, Oper. Res. **14**, 444 (1966); H. Stehfest, Commun. ACM **13**, 47 (1970); **13**, 624 (1970).

[21] F. J. Castaño, C. A. Ross, C. Frandsen, A. Eilez, D. Gil, H. I. Smith, M. Redjdal, and F. B. Humphrey, Phys. Rev. B **67**, 184425 (2003).

[22] M. C. Abraham, H. Schmidt, T. A. Savas, H. I. Smith, C. A. Ross, and R. Ram, J. Appl. Phys. **89**, 5667 (2001).